Polaramycin B, and not physical interaction, is the signal that rewires fungal metabolism in the Streptomyces – Aspergillus interaction.

Harald Berger[1], Markus Bacher[2,5], Roman Labuda[2,3], Isabel Maria Eppel[1], Florentina Bayer[1], Michael Sulyok[4], Erika Gasparotto[1,2], Franz Zehetbauer[1], Maria Doppler[4], Hannes Gratzl[2,4], Joseph Strauss[1,2, §]

Affiliations:

[1] University of Natural Resources and Life Sciences Vienna, Department of Applied Genetics and Cell Biology, Institute of Microbial Genetics, A-3430 Tulln/Donau

[2] Research Platform Bioactive Microbial Metabolites (BiMM), A-3430 Tulln/Donau

[3] Department for Farm Animals and Veterinary Public Health, Institute of Milk Hygiene, Milk Technology and Food Science; University of Veterinary Medicine Vienna, Veterinärplatz 1, 1210 Vienna, Austria

[4] University of Natural Resources and Life Sciences Vienna, Department of Agro-Biotechnology, Institute of Bioanalytics and Agro-Metabolomics, , A-3430 Tulln/Donau

[5] University of Natural Resources and Life Sciences Vienna, Department of Chemistry, Institute of Chemistry of Renewable Resources, , A-3430 Tulln/Donau

[§] corresponding author: Joseph Strauss, University of Natural Resources and Life Sciences Vienna, Department of Applied Genetics and Cell Biology, Institute of Microbial Genetics, University and Research Campus Tulln, Konrad Lorenz Strasse 24, A- 3430 Tulln/Donau, Austria, T:+43-1-47654-94420, E-Mail: joseph.strauss@boku.ac.at

Abstract

Co-culturing the bacterium *Streptomyces rapamycinicus* and the ascomycete *Aspergillus nidulans* has previously been shown to trigger the production of orsellinic acid (ORS) and its derivates in the fungal cells. Based on these studies it was assumed that direct physical contact is a prerequisite for the metabolic reaction that involves a fungal amino acid starvation response and activating chromatin modifications at the biosynthetic gene cluster (BGC). Here we show that not physical contact, but a guanidine containing macrolide, named polaramycin B, triggers the response. The substance is produced constitutively by the bacterium and provokes the production of ORS above a certain concentration. In addition, several other secondary metabolites were induced by polaramycin B. Our genome-wide transcriptome analysis showed that polaramycin B treatment causes down-regulation of fungal genes necessary for membrane stability, general metabolism and growth. A compensatory genetic response can be observed in the fungus that included up-regulation of BGCs and genes necessary for ribosome biogenesis, translation and membrane stability. Our work discovered a novel chemical communication, in which the antifungal bacterial metabolite polaramycin B leads to the production of antibacterial defence chemicals and to the up-regulation of genes necessary to compensate for the cellular damage caused by polaramycin B.

Introduction

Saprophytic fungi are dominant recyclers of natural organic substances specialized in breaking down recalcitrant plant material by their highly effective extracellular enzyme system. However, competition for nutrients, water and space by other organisms such as bacteria may urge fungi to produce defence or signalling compounds, for example antibiotics or other toxic compounds, collectively known as

68 secondary metabolites (SMs), that supress competitors (De Boer et al., 2005; Rousk and Bååth, 2007;
69 de Menezes et al., 2017). The same principle is used by pathogenic fungi which use both extracellular
70 proteins and an arsenal of toxins to penetrate host cells and supress defence mechanisms, respectively
71 (Doehlemann et al., 2017). Apart from their toxic properties, some of these substances are also known
72 to serve as signalling molecules, e.g. for fungal reproduction (Rodriguez-Urra et al., 2012),
73 establishment and maintenance of endophytic or symbiotic associations (Chujo et al., 2019) or
74 pathogenesis-related effectors (Boenisch and Schäfer, 2011; Pusztahelyi et al., 2015). Each fungal
75 species contains genes coding for the biosynthesis of many different SMs but at a given environmental
76 or developmental condition only a specialized set of these secreted molecules is produced. This
77 condition-specific metabolic signature is regulated by genetic signalling networks that have evolved as
78 energy-saving modules for these demanding biosynthetic processes (Yu and Keller, 2005; Gacek and
79 Strauss, 2012; Macheleidt et al., 2016). In many cases the signal triggering transcriptional activation of
80 the biosynthetic genes is connected to nutrient starvation or the onset of reproductive development
81 (Tag et al., 2000; Nemeth et al., 2016). But there are other examples in which rich nutrient sources and
82 active growth is correlated with the production of SMs, such as for the production of siderophores that
83 are required for iron acquisition and metabolism (Oberegger et al., 2001).

84 The biosynthetic pathways for these metabolites usually encompass many different enzymatic steps
85 and it is a striking feature that biosynthetic and regulatory genes as well as genes encoding transport
86 proteins of a given SM are usually clustered in the genome (termed "biosynthetic gene clusters", BGCs)
87 and transcriptionally co-regulated. Co-regulation is achieved by cis-acting elements targeted by
88 pathway-specific and broad-domain transcription factors, as well as by chromatin level regulation
89 which facilitates or inhibits access of these regulatory complexes to the target region (Keller et al.,
90 2005; Strauss and Reyes-Dominguez, 2011; Brakhage, 2013). One of the main conclusions drawn from
91 the analyses of the ever-increasing fungal genome databases is the discrepancy between known
92 metabolites and the number of predicted BGCs. For each of the sequenced species, usually only a few
93 SMs are known but many more BGCs are predicted in their genomes (Li et al., 2016). This is not only
94 true for less-studied species but even in aspergilli or penicillia only 20%-30% of the theoretically
95 existing and predicted chemical diversity is known. Taken together this indicates that the majority of
96 BGCs are not expressed under the usually employed standard laboratory growth conditions and we
97 still are not able to mimic the full diversity of growth and developmental conditions that would trigger
98 the production of the full array of metabolites in any of the studied organisms.

99 One of the triggers that received high attention recently is biotic interactions. It is known since a long
100 time e.g. for pathogenic fungi like *Fusarium graminearum*, that a high proportion of predicted BGCs is
101 only expressed during pathogenic growth (Desjardins et al., 1993; Boenisch and Schäfer, 2011). The
102 corresponding transcriptional program responds to the encountered plant material (substrate

103 response) and to the plant defence system (active plant response). Each of these conditions activates
104 a different subset of SMs in *F. graminearum* (Boedi et al., 2016). There are numerous examples in
105 which biotic interactions of a pathogenic, symbiotic or endophytic life style alters the secondary
106 metabolome of the fungal interaction partner. Also, free-living interactions have been found to alter
107 the SM profiles, e.g. in the mutual interaction between the soil inhabitants *Aspergillus nidulans* and
108 *Streptomyces rapamycinicus* (Schroeckh et al., 2009). In this case, *A. nidulans* produces orsellinic acid
109 (ORS) and yellow polyketides (YPKs), SMs that are barely found in axenic cultures under standard
110 laboratory growth condition (Sanchez et al., 2010). The bacterial trigger ultimately leads to an
111 activating chromatin landscape at the corresponding ORS/YPK BGC (Nützmann et al., 2011) and the
112 formation of this open chromatin structure depends on the function of BasR, a fungal transcription
113 factor induced by amino acid starvation (Fischer et al., 2018b). Consistent with a chromatin-level
114 regulation of the ORS/YPK cluster the same activation can be observed in mutants lacking CclA or
115 KdmB, central components of complexes which regulate the methylation status of histone H3 lysine 4
116 (Bok et al., 2009; Gacek-Matthews et al., 2016). Also, the addition of the non-metabolizable histidine
117 analogue 3-aminotriazole (3-AT) leads to ORS/YPK induction indicating that the intimate fungal-
118 bacterial contact is not mandatory but bacterial cells or their metabolites may function via an amino
119 acid starvation response and so-far uncharacterized downstream signalling cascades that eventually
120 lead to BasR-mediated chromatin activation (Fischer et al., 2018). How BasR function is connected to
121 the histone H3K4 methylation/demethylation machinery remains to be uncovered.

122 Using a particular experimental set-up, we identified a specific bacterial macrolide, known as
123 polaramycin B, that is able to trigger ORS/YPK production in *A. nidulans* also in the absence of bacterial
124 cells. We performed RNA-sequencing to test whether polaramycin B application is equivalent to the
125 direct physical contact between the fungal and bacterial cells and found that it fully mimics the
126 transcriptional and metabolic response of the organismic interaction. Strikingly, only Streptomyces
127 species carrying the predicted BGC for guanidine-containing macrolides are able to induce the fungal
128 response.

129

130

131 ## Results

132 ### The supernatant of *S. rapamycinicus* is sufficient to induce yellow pigment and
133 orsellinic acid production

134 To better understand the interaction between *A. nidulans* and *S. rapamycinicus*, we set up an
135 experimental system that allowed us to differentiate fungal hyphae directly interacting with *S.*
136 *rapamycinicus* from non-directly interacting fungal cells. This setup used fungal and bacterial cultures
137 grown on solid surface in contrast to the previously applied conditions of co-culturing them in liquid

138 shake flasks. In the actual approach the fungal and the bacterial colonies were inoculated at opposing
139 sides of a Petri-dish that contained only agar without nutrients. To allow for some limited growth of
140 the inoculated fungal and bacterial cells, the points of inoculation were supplied with nutrients. This
141 set-up produced a thin, low-density fungal colony spreading out over the agar surface and this allowed
142 us to easily observe colour or morphological changes of the colonies. Figure 1A top shows an example
143 of the experiment in which fungal inoculation points were fed with AMM and bacterial inoculation
144 points with M79 media. Starting from these nutrient reservoirs at the opposite sides of the Petri dish
145 the organisms were able to grow into the nutrient-free agar. Using this setup, we observed that fungal
146 mycelium spreading from at the opposite side towards the bacterial colony was producing some yellow
147 pigments (YPs) although there was no direct contact yet with the *S. rapamycinicus* colony (Figure 1A).
148 No colour changes at the *A. nidulans* mycelia were observed in control experiments growing the fungal
149 cells alone. These observations indicated that yellow polyketides and orsellinic acid may be produced
150 by *A. nidulans* cells in response to the presence of *S. rapamycinicus* already before their physical
151 contact takes place. To make sure there is no direct interaction via buried bacterial or fungal cell
152 interactions we used a similar setup but containing *S. rapamycinicus* cells within a dialysis tube. The
153 molecular weight cut off 8.000-10.000 kDa allowed nutrients passing through the membrane at the
154 point of inoculation but prevented bacterial cells to spread on or through the agar. We found also in
155 this setup an induction of YPs (Figure 1B). To test if the signal for fungal pigment production requires
156 actively growing bacterial cells or if a bacterial metabolite may be sufficient to induce YPs we
157 subsequently applied sterile-filtered culture supernatant from a *S. rapamycinicus* liquid culture grown
158 in M79 media without *A. nidulans*. When adding these bacterial culture supernatants to an *A. nidulans*
159 colony growing alone on the nutrient-free agar we also observed YP production, although colouration
160 was less intense (Figure 1C). Since in this latter approach *S. rapamycinicus* was grown "solo" without
161 *A. nidulans*, we could conclude that production of the YPs in *A. nidulans* is triggered by one or more
162 compounds secreted by *S. rapamycinicus* cells growing in M79 medium and that the production of this
163 inducer(s) does not depend on the presence of a competing or interacting organism. However, the
164 presence of a competing organism like *A. nidulans* may cause elevated production of this unknown
165 molecule(s).

166 Yellow pigment (YP) production correlates with metabolites from the orsellinic acid 167 pathway

168 As the direct physical *A. nidulans* - *S. rapamycinicus* interaction was shown to trigger the production
169 of ORS and YPs, we then tested if production of the pigments in our test system indeed correlate with
170 these metabolites. For chemical analysis a similar, but larger size set-up of our nutrient-free agar
171 cultivation assay was used (petri dishes with 15 cm diameter) where we grew the organisms for 7 days.
172 Subsequently, in a 9 x 4 grid, agar blocks of 1 cm x 1 cm size were cut out, extracted and metabolites

173 within these agar-blocks were subsequently analysed via photometric absorption measurements at
174 400nm and by HPLC-MS (Figure 2A and supplementary Figure S1).

175

176 Results of this chemical analyses showed that several metabolites of the ORS biosynthetic pathway
177 were detectable in the extracts obtained from agar samples derived directly from, or from the vicinity
178 of the *A. nidulans* cells growing towards the *S. rapamycinicus* colony. The concentrations of ORS as
179 well as lecanoric acid (LEC) showed strong correlation with the absorption at 400nm that visually
180 appears as yellow colour (Spearmen rho: 0.72 and 0.70 for ORS or LEC, respectively, with p-values of
181 6.36E-7 or 1.52E-6, see also correlation plot in supplementary Figure S2). These data indicated that our
182 macroscopically observed YPs actually contain ORS and LEC. Additional fungal metabolites have been
183 found in the analyzed agar blocks (Figure 1S). Some of them are also found in higher quantities in the
184 competition zone between fungal and bacterial colonies, but others are more abundant in blocks
185 excised from regions outside of the competition zone.

186 Interestingly, also *S. rapamycinicus* metabolites seem to be induced by the presence of the fungal
187 mycelium, e.g. terragine is clearly more abundant in the competition zone between the two organisms
188 than anywhere else in the agar of the petri dish. On the other hand, production of the fungal
189 diketopiperazines cyclo(L-Pro-L-Tyr) and cyclo(L-Pro-L-Val) are apparently repressed by the interaction
190 and they show a comparatively lower abundance in this zone (see Figure2 and supplementary Figure
191 S1).

192 Taken together, our experiments showed that an active communication based on secreted metabolites
193 takes place between these two organisms and that the cellular responses do not dependent on
194 physical interaction among them. Different concentrations of specific secondary metabolites at
195 different locations within the whole growth area moreover indicate that fungal and bacterial
196 metabolites can be induced or repressed by the chemical signals generated by the cultures.

197

198 The inducer of YPs comprising orsellinic and lecanoric acid is a guanidine-containing
199 polyhydroxyl macrolide

200 To identify the metabolite(s) from *S. rapamycinicus* inducing YPs in *A. nidulans* we grew *S.*
201 *rapamycinicus* in the absence of fungal cells "solo" in in M79 medium for 7 days and used a sterile-
202 filtered culture supernatant for the development of an *A. nidulans* bioassay that would monitor YP
203 induction. The fungal bioassay was based on miniature cultures in a 24 well microtiter plate (MTP)
204 format where we grew *A. nidulans* colonies in submerged cultures and were able to use simple colour
205 change of the medium as an indicator of YP production (see details in methods and materials). Using
206 this assay we could confirm that the supernatant of *S. rapamycinicus* cultures were indeed inducing YP

207 in *A. nidulans* and thus can be used for bioassay-guided fractionation tests. Subsequently, several
208 liquid-liquid extraction methods (n-Hexan, Dichlormethan, Acetonitril) were tested and we found that
209 the YP inducer always remained in the aqueous phase indicating that it is a polar substance that may
210 be extractable with methanol. Finally, *S. rapamycinicus* was grown massively on M79 agar plates and
211 the methanol extracts were then further fractionated successively using flash column chromatography
212 and preparative high performance liquid chromatography (HPLC). All fractions were then tested in the
213 bioassay for YP-inducing activity. A highly pure fraction was obtained and purified by preparative HPLC.
214 Subsequent structural elucidation of the active fraction by HPLC-MS/MS and NMR identified the
215 guanidine-containing polyhydroxyl macrolide polaramycin B as the YP, i.e. ORS and LEC inducing
216 compound.

217 Polaramycin B biosynthetic gene cluster prediction

218 To bioinformatically identify the so far uncharacterized polaramycin biosynthetic genes, we performed
219 antiSMASH (Medema et al., 2011) searches of 6 different Streptomyces strains including *S.*
220 *rapamycinicus*, *S. lateritius*, *S. zaomyceticus*, *S. ederensis*, *S. europaeiscabiei* and *S. iraniensis* based on
221 published genome sequences and annotations. As polaramycin is similar to azalomycin, a well-
222 characterized guanidine-containing macrolide, we assumed that similarity to the known azalomycin
223 biosynthetic gene cluster (BGC) would be indicative for a BGC potentially responsible for polaramycin
224 production. Only in *S. rapamycinicus* and *S. iraniensis* a homology with the azalomycin F3a biosynthetic
225 gene cluster from Streptomyces sp. 211726 (MIBiG accession: BGC0001523) could be detected (Figure
226 4). To substantiate the hypothesis, we also cultivated isolates of four additional Streptomyces species
227 under identical conditions as done before for *S. rapamycinicus*. Strikingly, only the two species *S.*
228 *rapamycinicus* and *S. iranensis*, which contained the predicted gene cluster similar to the azalomycin
229 cluster in their genomes, induced YP production. In contrast, the other four species not harbouring
230 these BGCs showed no YPs (see supplementary Figure S3). These findings suggest that the region
231 showing homology to the azalomycin biosynthesis cluster is responsible for the production of
232 polaramycin in *S. rapamycinicus* and *S. iraniensis* and thus for YP induction.

233

234 Dose Response of polaramycin B

235 Since induction of orsellinic acid production was previously only observed when *S. rapamycinicus* and
236 *A. nidulans* interacted physically, we reasoned that in these former liquid shake co-cultures the local
237 concentration of polaramycin B at the fungal cell surface may not have been sufficiently high to induce
238 the metabolic changes. In this former set-up, the concentration necessary to trigger ORS induction may
239 only have been reached when cells directly interacted with each other because this physical interaction
240 prevented immediate diffusion of the inducer away from the fungal cell surface. We therefore tested
241 YPs production and *orsA* gene expression in *A. nidulans* cultures treated with different concentrations

242 of polaramycin B in our 24 well plate bioassay. We found that after 48 hours of incubation a
243 concentration of 0.5 µg/mL polaramycin B in the *A. nidulans* growth medium is necessary to induce
244 YPs as well as *orsA* transcription (Figure_S4). This concentration was then used in our genome-wide
245 transcriptional analysis aimed at determining whether polaramycin B treatment induced a similar
246 genetic response as previously observed in the physical interaction and if other fungal secondary
247 metabolites are also affected by the addition of polaramycin B treatment. Moreover, the identification
248 of transcriptional network changes by the treatment is of interest to understand which fungal targets
249 are affected by this compound.

250 Polaramycin B induces the dba1-dba2 gene cluster for ORS biosynthesis

251 For RNA-seq analysis, we used *A. nidulans* cultures pre-grown for 18 hours in AMM shake cultures and
252 subsequently added polaramycin B at a concentration of 0.5 µg/ml. As the transcriptional network
253 changes triggered by the substance may differ depending on the duration of treatment, we chose two
254 different harvesting times. To test for the short-term response, we harvested the mycelia after 30
255 minutes of incubation and for the response to an extended treatment time the cultures were harvested
256 after 3 hours of incubation with polaramycin B. It needs to be mentioned that at this time point there
257 is still 0.45- 0.5% glucose remaining in the AMM medium, a concentration that is known to repress
258 starvation-induced secondary metabolites, such as the production of sterigmatocystin. To control if
259 under these conditions polaramycin B also induces YPs and ORS, we first tested the expression levels
260 of *orsA* (AN7909), the polyketide synthase-encoding gene. Using RT-qPCR we could confirm the
261 induction event (data not shown) and we thus used these samples for RNA sequencing via Illumina Hi-
262 Seq.

263 In respect to the ORS gene cluster our data analysis showed that the genes of the split dba1-dba2
264 cluster are induced by polaramycin B treatment. Moreover, the regulatory gene *dbaA,* which encodes
265 the specific transcription factor of this BGC, and which resides within the dba1 cluster, is induced
266 already after 30 minutes. Consistent with DbaA being the cluster-specific transcriptional activator
267 protein, other genes within the dba1-dba2 BGC, were found to be induced after three hours post-
268 treatment. Interestingly, one gene of unknown function (AN7913, designated *orsD*) and located within
269 the dba2 region also shows the same induction kinetics as the transcription factor (induction after 30
270 minutes). Other dba1 cluster genes residing in the neighbourhood of the *dbaA* transcription factor
271 gene also seemed to be induced after 30 minutes. This result that may hint towards a local chromatin
272 effect that renders the *dbaA*-containing region transcriptionally active.

273 Polaramycin B also induces other BGCs

274 Our transcriptome data allowed to analyse whether other BGCs were also affected by the polaramycin
275 B treatment. Indeed, we found that several other BGCs are also changed in their transcriptional

276 activity. For example, a majority of genes in the terrequinone (Bouhired et al., 2007) or aspercryptin
277 (Henke et al., 2016) BGCs are significantly upregulated. Some BGCs showed only partial activity, such
278 as the asperfuranone or the AN10289 cluster (Klejnstrup et al., 2012), in which only roughly half of the
279 predicted cluster genes are induced. Interestingly the penicillin cluster, whose 3 genes are already
280 transcribed at intermediate levels in our overnight cultures, are significantly downregulated by
281 polaramycin B treatment (see Table 1). Thus, apart from the YPs and few other substances, the
282 majority of BGCs do not show significant alterations in their expression profiles. This transcriptional
283 response is similar to what has been also observed in the previous experiments in which *A. nidulans*
284 cells experienced direct physical contact with *S. rapamycinicus* (Schroeckh et al., 2009). These findings
285 indicate that polaramycin B is the responsible substance that mediates the transcriptional response of
286 A.nidulans in the *S. rapamycinicus* interaction.

287

288 The induction kinetic suggests possible modes of action of polaramycin B

289 We have been involved in the elucidation of the BasR and chromatin-based mechanisms by which *S.*
290 *rapamycinicus* changes the *A. nidulans* metabolism during their physical interaction (Fischer et al.,
291 2018a). To identify putative targets of polaramycin and analyse the possible overlap between physical
292 interaction and chemically triggered responses, the transcriptional profiles were grouped into 8
293 clusters (see Figure 6): Immediately upregulated to steady state (A1); Immediately downregulated to
294 steady state (A2); Immediately upregulated and continuously further upregulated (B1); Immediately
295 downregulated and continuously further downregulated (B2); Delayed upregulated (C1); Delayed
296 downregulated (C2); transiently upregulated (E1); transiently downregulated (E2).

297 A significant regulation was assumed if absolute log2 difference was greater than 1 and p-value was
298 less than 0.01. The contrasts considered were between time point zero and 30 minutes as well as
299 between 30 minutes and 3 hours. In case of disagreement between log2 difference and p-value no
300 differential regulation was assumed. To identify processes possibly involved in the polaramycin
301 response we searched for overrepresented gene ontology (GO) annotations in each gene-set
302 (Ashburner et al., 2000).

303 Genes immediately responding to polaramycin B treatment

304 Interestingly, in the gene-set of genes "immediately upregulated to steady state " (A1, 151 genes) GO
305 annotations associated with translation or ribosome biosynthesis were significantly overrepresented.
306 The genes with these annotations in cluster A1 were already transcribed at intermediate levels but
307 polaramycin B caused a significant increase at least 2 fold.

308 In addition to the translation process, also few genes putatively associated with membrane stability
309 and function are found in this immediately induced gene set like AN3125 (predicted role in response

310 to stress and integral to membrane localization), AN7327 (predicted glycosylphosphatidylinositol GPI-
311 anchored protein), AN9342 (predicted role in transmembrane transport and integral to membrane
312 localization) among the highest differentially expressed genes.

313 In the gene-set of genes "immediately downregulated to steady state" (A2, 236 genes) the GO
314 annotation "Lipid metabolic process" was significantly enriched which supports the findings that the
315 antifungal activity of macrolides (like Azalomycin F) is based on disturbance and leakage of the
316 phospholipid cell membrane (Sugawara, 1967). But in our experiments we found only few genes
317 differentially regulated with the GO annotation "Response to osmotic stress" (e.g. AN065) which could
318 be a hint that the cell membrane disturbance caused by polaramycin B has no large impact or can be
319 well counteracted by the fungal metabolism, such as by those induced genes mentioned above coding
320 for membrane stability functions.

321 The rather small gene-set B1 of genes "immediately and continuously upregulated" (22 genes) mainly
322 contains the upregulated BGCs, such as 2 genes from the dba-cluster and 3 genes from the AN7884-
323 cluster (aspercryptin) as well as one from the AN0016-cluster (*pes1*). Statistically, no significant GO-
324 term enrichment could be detected what may be due to the small size of this gene-set.

325 Also the gene-set B2 of genes "immediately and continuously downregulated" is rather small (16
326 genes) and contains mainly transport-related genes. For example, AN9168 (putative solute-hydrogen
327 symporter activity with role in glycerol transmembrane transport), AN6277 (predicted role in
328 transmembrane transport), AN4277 (putative glucose transmembrane transporter activity), AN3489
329 (putative endoplasmic reticulum localization) and AN6071 (domains with predicted membrane
330 localization) are found in this gene set.

331

332 Genes only responding to extended polaramycin B incubation

333 We could observe that a larger number of genes is only differentially expressed after prolonged
334 treatment with polaramycin B. These genes were grouped into sets C1 and C2 comprising of 638
335 upregulated and 573 downregulated genes. The upregulated gene-set C1 showed no concise picture
336 in respect to enriched GO-terms but next to a diverse array of predicted gene functions, it contained
337 basically all upregulated BGCs discussed above. Most of the dba-cluster genes fall into this C1 gene-set
338 as well as several other secondary metabolite cluster genes(see Table 1) In addition to BGCs, some of
339 the strongest induced genes have a linkage to oxidative stress responses, like AN7893, which has
340 predicted oxidoreductase activity, AN9315 has a role in NADH oxidation and regulation of reactive
341 oxygen species, AN5397 is a copper-containing laccase that oxidizes phenolic substrates or AN2559
342 with predicted nucleotide binding and oxidoreductase activity. The fact that these genes are
343 upregulated upon prolonged polaramycin B treatment may be a result of a disturbed membrane

344 potential triggered by the substance eventually causing oxidative stress. If this stress is the "real"
345 inducer of YPs remains to be determined.

346 Predicted functions of genes downregulated upon prolonged polaramycin treatment (gene set C2) are
347 associated with GO terms like hyphal growth, DNA replication or cell cycle regulation. This indicates
348 that polaramycin B treatment impairs growth processes, a result that we have already observed in our
349 phenotyping plate assays (Figure 1 and 2).

350 As can be seen in Figure 6 for the gene-set C2 general catabolism related GO terms fall into this
351 category. These include AN7180 and AN7541, which are two cutinases involved in carbohydrate
352 catabolism, AN11188 with a putative role in endocrocin biosynthetic process, AN2719 with cell wall
353 peptidoglycan catabolic process, AN11159 with phospholipid biosynthetic process. Also, many
354 proteolytic or hydrolytic enzymes are found in this gene-set: AN7121 (predicted
355 metallocarboxypeptidase), AN5558 (alkaline protease), AN111981 (predicted UDP-N-acetylmuramate
356 dehydrogenase), AN1583 and AN0009 (predicted hydrolase), AN3393 (similarity to neutral
357 metalloprotease II), AN7962 (deuterolysin-type metallo-proteinase), AN8445 (Putative
358 aminopeptidase). The complete list of genes is shown in supplementary Table ST2. The downregulation
359 of these hydrolytic enzymes may be a result of the reduced growth probably to avoid self-digestion or
360 a reduced turnover of metabolites to not allow potential competitors to feed easily on such generated
361 metabolites.

362

363 Genes with a transient response to polaramycin treatment

364 There are genes that have a strong short-term response to the treatment with polaramycin B
365 (measured after 30 minutes exposure) but this response is lost upon prolonged treatment with the
366 drug (measured after 3 hours exposure) Gene-set D1 holds 54 genes which are immediately
367 upregulated by the presence of polaramycin B but no response is observed any more in the 3 hours
368 treatment cultures. No clear picture comes out from this gene set but 2 GPI- anchored proteins
369 (AN7792 a Putative lysophosphoplipase A and AN8609), AN2798 (predicted role in response to stress
370 and integral to membrane localization), AN0209 (mepB, High-affinity ammonium transporter), AN4372
371 (*pgaB*, a protein with polygalacturonase activity) have been found in this gene-set. This may hint
372 towards a reaction on the membrane due to polaramycin B that is transient as the cell may be able to
373 balance the membrane defects after the respective genes have been induced and new membrane
374 components have been produced.

375 Also, quite a significant number of genes were found to be transiently repressed by polaramycin B
376 treatment. 90 genes were found in this set of genes designated D2 (Figure 6). Interestingly 3 genes

377 associated with trehalose, an important storage carbohydrate in fungi are in this gene-set, AN9340
378 (*treA*), AN10533 and AN5523 (*tpsA*). Since trehalose plays also an important role in conidial stability,
379 this may be a reflection of the dynamics following the immediate downregulation of carbohydrate
380 metabolic processes (see gene-set A2) post polaramycin B treatment

381

382 ## Discussion

383 ### Polaramycin B structure, function and concentration thresholds for changing fungal
384 metabolism.

385

386 The molecular details of the interaction between microorganisms that compete for physical space
387 and/or metabolic resources is still a relative sparsely investigated field of molecular microbiology
388 despite its omnipresence in our biosphere. In previous work it was suggested that a direct, physical
389 contact between *S. rapamycinicus* and *A. nidulans* is necessary to trigger the genetic response of the
390 fungus leading to the production of orsellinic acid (ORS) and its derivates (Schroeckh et al., 2009b).
391 Using a novel experimental system, we were now able to identify the chemical molecule that triggers
392 the genetic response underlying the ORS production in these co-cultures. We identified a 36 carbon-
393 membered polyol macrolide containing a hemiacetal monoester of malonic acid and a guanidyl group,
394 collectively known as polaramycin B. This substance has previously been extracted from *Streptomyces*
395 *hygroscopicus* LP-93 but to the best of our knowledge not much research has been done on this
396 particular variant of guanidine-containing polyhydroxyl macrolide since its discovery in 1997 (Meng
397 and Jin, 1997).

398 Generally these macrolides have been shown to possess broad-spectrum antibacterial and antifungal
399 activities (reviewed in (Song et al., 2019)). By comparison of different variants of these macrolides, the
400 following assumptions about structure-function relationships could be made: The size of the lactone
401 ring has minor influence on the antimicrobial activity (32 and 36 sized structures were compared), but
402 the terminal guanidine group is crucial for their antibacterial and antifungal activities. The six-
403 membered hemiketal ring (C17-C21) plays an essential role in the antimicrobial activity, the malonyl
404 group (C23) reduces the antimicrobial activity and reduction of double bond or methylation of the
405 lactone ring does not have a strong influence on the antimicrobial activity (see (Song et al., 2019) and
406 references therein).

407 Most likely, in many natural environments the concentration of polaramycin B will not reach or exceed
408 the threshold concentration of 0.5µg polaramycin B per ml of medium, as determined in the artificial
409 laboratory growth condition. Therefore, in nature, direct interaction between bacterial and fungal cells
410 will most likely still be required for effective chemical communication, simply because the triggering

411 molecules freely diffuse. And this may also have been the reason why in high-volume liquid shake co-
412 cultures the required concentration of polaramycin B was only reached when cells directly interacted.
413 Also, the fungal cell density plays a role as higher cell densities dilute the number of polaramycin B
414 molecules per fungal cell. We conclude this because in densely growing *A. nidulans* cultures incubated
415 on high-nutrient AMM culture plates (55 mM glucose, 10mM nitrate) the YPs-inducing effect by
416 opposing *S. rapamycinicus* colonies was very hard to observe compared to the water-agar medium
417 lacking these nutrients. In the latter, YPs were easily detectable in the very fine and thin mycelial
418 network that *A. nidulans* cells develop under these conditions.

419 The metabolic response of fungal colonies to bacterial confrontation is unidirectional.

420 The water-agar plate assays allowed us to observe the metabolic "warfare" between the two
421 microorganisms and we could observe that the fungal colony produces YPs and ORS only in the region
422 that faces the bacterial colony, but not in the far side and in distant areas of this competition region.
423 That indicates that the fungal cells respond individually to the presence of the bacterium and that this
424 signal is not transferred very far through the mycelial network. So, a fungal colony only seems to
425 represent a limited "information network" that does not lead to a genetic alert of cells not directly
426 connected to each other. Macroscopically, a fungal colony appears as an interwoven network of cells,
427 however, most likely at the cellular level, they may not be truly connected as one would expect distant
428 cells of a colony also responding to the presence of polaramycin B in a similar way the cells facing the
429 confrontation zone, do. Apart from the observed production of YPs and other secondary metabolites,
430 this spatially limited response was also observed for other phenotypic changes caused by polaramycin
431 B, such as a lack of growth inhibition and onset of sporulation at the distant, far side of the competition
432 zone. The conidiation phenotype was corroborated with data from our transcriptome analyses in
433 which we observed highly transcribed sporulation related genes (e.g. AN3624 (*ygA*), AN4998(*gapA*),
434 AN2513 (*pipA*), AN0928, AN7735 (*eglD*) and AN0863 after polaramycin B treatment. This observation
435 indicates that a fungal colony, although representing a network of connected cells, does not represent
436 an "information network" in the sense that a signal arriving at one end of the colony is passed on to
437 the other side of the same colony.

438 Possible mode of action of polaramycin B

439 Beside the dba1-dba2 cluster for ORS and YPK production, also other BGCs showed increased
440 transcription levels in response to polaramycin B. These included aspercryptin and the terrequinone
441 clusters, but due to lacking metabolite standards, missing mass-spectrometry data or low metabolite
442 concentrations the clear-cut correlation between transcriptional levels and metabolite concentrations
443 cannot be made at the moment. On the other hand, not all *A. nidulans* BGCs seem to respond equally
444 to polaramycin B treatment. For example, the penicillin cluster in is repressed by this substance. This
445 is interesting in light of the fact that Streptomycetes strains are known producers of penicillin and

446 similar antibiotics. Therefore, these bacteria require a strong self-resistance mechanism against these
447 types of antibiotics and apparently, *A. nidulans* actively ceases production of an antibiotic that is
448 obviously useless against this specific competitor (reviewed in (Ogawara, 2016)).

449 Previously, it has been shown that a closely related molecule to polaramycin B, azalomycin F, acts on
450 fungi via disturbance of the cell membrane, but not much work was committed into deciphering its
451 mode of action. We applied transcriptomics to gain more insight and could identify genes related to
452 lipid metabolism, membrane function and growth regulation as being down-regulated during the
453 treatment. Apparently, affected cells responded to this challenge by up-regulation of possible
454 compensatory genetic networks, such as genes necessary for membrane stability, for translation and
455 ribosomal functions as well as enzymes that counteract oxidative stress. This response overlaps with
456 the 3-Amino-triazol (3-AT) treatment and is also similar to the response of the direct physical
457 interaction between *A. nidulans* and *S. rapamycinicus*, (Nützmann et al., 2011; Fischer et al., 2018a).
458 3-AT exposure is known to block histidine biosynthesis eventually leading to an amino acid starvation
459 and induction of the cross-pathway control genes like *cpcA* and *basR* (Braus et al., 2006*)*. Our groups
460 also found chromatin mutants with changes in the ORS and YPs production.

461 A chromatin-related function of polaramycin B in activating BGCs?

462 Chromatin structure is influenced by histone modifications and in fungi, transcriptional co-regulation
463 of the genes residing inside a certain BGC, is facilitated by chromatin transitions (Strauss and Reyes-
464 Dominguez, 2011; Pfannenstiel and Keller, 2019). Interestingly, a mutant lacking a component of the
465 COMPASS complex that is responsible for activating histone H3K4 methylation (H3K4me3) was found
466 to strongly overproduce ORS and YPKs and also featured strongly induced expression of the dba1-dba2
467 cluster (Bok et al., 2009). Consistently, the opposite type of mutant lacking the H3K4me3 de-methylase
468 gene KdmB, showed lower expression of these BGCs (Gacek-Matthews et al., 2016; Bachleitner et al.,
469 2019). As H3K4me3 is a histone modification generally associated with activating functions, it seems
470 counter-intuitive that a mutant lacking this function would be more active in transcription of the
471 ORS/dba cluster. However, it is known that cells lacking the H3K4 methyltransferase system have a
472 defect in silencing loci positioned at or near chromosome (Nislow et al., 1997; Margaritis et al., 2012).
473 Additionally, or alternatively, the lack of H3K4 methylation may downregulate a basic metabolic gene
474 involved in amino acid biosynthesis thus leading to amino acid starvation and subsequent induction of
475 ORS/YPs production. The experimental proof of this hypothesis awaits further research.

476 Materials and Methods

477 Strains and cultivation conditions for transcriptomics

478 Aspergillus nidulans WT (pabaA1 veA1) was the fungal strain used throughout the study (Pontecorvo
479 et al., 1953). *Streptomyces rapamycinicus* strain was the one used by Fischer *et* al. in our laboratory

480 for the transcriptome and chromatin analysis (Fischer et al., 2018). Conidiospores from cryostocks
481 were plated on Aspergillus minimal medium (AMM) plates (10mM nitrate, 1% Glucose, 15 pM para-
482 amino benzoeic acid), incubated for three days at 37 °C and harvested in autoclaved deionized water
483 (diH2O) containing 0.1 % Tween-20. A spore density of 1E6 spores/mL was inoculated in 50 mL of liquid
484 AMM in 100 mL Erlenmeyer flasks, respectively, and the culture grown at 37 °C and 180 rpm. The time
485 of cultivation was 18 hours. Treatment with polaramycin B (0.5µg/ml) for 30 minutes and 3 hours or
486 no treatment was applied.

487 Starvation plate assay

488 Starvation plates were agar plates containing only AMM salts without nutrients (0.52g/l KCl, 0.815g/l
489 KH2PO4, 1.045g/l K2HPO4), 2 circular regions (diameter: 15 mm) were cut out and filled with AMM-
490 or M79-agar and inoculated with 1 µl of Aspergillus or Streptomyces spore suspensions (5E6 and 5E8
491 spores /ml) , respectively. For metabolite analysis 1x1x0.5 cm agar blocks were cut out and metabolites
492 were extracted in 3 ml Acetonitril-Acetic acid-Water (79:1:20) solvent.

493 Bioassay

494 The bioassay to detect yellow pigment production in *A. nidulans* was designed for 24 well plates. 1E+6
495 *A. nidulans* spores were incubated per ml AMM and grown in submerse culture in 50 ml AMM at 30°C
496 shaking (180rpm) flask overnight. Single fungal pellets were placed in wells of a 24 well plate and 2ml
497 of AMM media not containing trace elements was added. The plate was then incubated for 2-3 days
498 at 37°C. No sporulation could be observed till this time points. These plates were then used for testing
499 extracts.

500 Streptomyces fermentation

501 Liquid fermentation of *Streptomyces rapamycinicus* was performed in M79 medium using 1E+7
502 spores/ml in 50 ml at 30°C 160rpm. Solid state fermentation was performed on M79 agar plates (10g/l
503 Glucose, 10g/l bacto-peptone, 1g/l casamino acids, 2 g/l yeast extract, 6 g/l NaCl, pH 7.2). For the final
504 polaramycin B preparation 2000ml M79-agar was distributed into 40 petri-dishes (large) and each one
505 inoculated with 1E+7 spores/plate. After 7 days of growth at 30°C agar was cut into approximately 1cm
506 x 1cm pieces and extracted with 1.5 L methanol over night at room temperature. The filtered methanol
507 fraction was then evaporated to a volume of 5ml.

508 Isolation of the macrolide

509 The crude extract was purified by reversed-phase silica gel vacuum flash chromatography (Interchim,
510 puriFlash®450), using three consecutive Interchim puriFlash® 32 g silica IR-50C18-F0025 flash columns
511 (particle size: 50µm). The columns were eluted with a binary solvent gradient (solvent A: H2O, solvent
512 B: ACN). The starting linear gradient from 10% B to 27% B during 25 min at a flow rate of 15 mL/min

513 was followed by an isocratic elution at 52% B for 10 min. Then a linear gradient from 52% to 66% B
514 over 7min was applied at the same flow rate and finally the column was washed starting with 100% B
515 for 10 min followed by 100% A for 10 min at a flow rate 15-30 mL/min. UV 254 nm and UV scan 200-
516 400 nm modes were used for detection and final separation of 8 main fractions (F1-F8), which were
517 consequently concentrated under reduced pressure at 45°C. The target compound (activity) was found
518 in fraction F5 (18-20 Rt, yield: 25 mg).

519 This fraction was further dissolved in 1:1:1; ACN/CH3OH/H2O and purified by an Agilent 1260 Infinity
520 preparative HPLC (USA) on a reversed phase column Gemini NX C-18 (21.20 x 150 mm, 5 µm, 110 Å).
521 Gradient starting with 30 % ACN and 70 % H2O up to 95 % ACN in 32min (total time 45 min) and a flow
522 rate of 25 ml/min. Four preparative fractions (pF1 -pF4, bioactivity guided fractionation, time lapse
523 fractionation) were collected, of which pF3 was found as active. The active fraction was further
524 proceeded with 2nd stage prep HPLC (signal lapse fractionation). The active signal (target) was found
525 at tR 10.5 min, yielding 0.91mg. For purity check an Agilent 1200 system was used with the same
526 stationary phase and gradient program.

527 Secondary metabolite and Orsellinic acid quantification

528 Metabolite analysis was carried out using a 1290 Series HPLC System (Agilent, Waldbronn, Germany)
529 coupled to a QTrap 5500 LC-MS/MS System (Applied Biosystems SCIEX, Foster City, CA) equipped with
530 Turbo Ion Spray electrospray ionization source as described earlier (Sulyok et al., 2020).
531 Chromatographic separation was performed at 25 oC on a Gemini® C18-column, 150 x 4.6 mm i.d., 5
532 µm particle size, equipped with a C18 4 x 3mm i.d. security guard cartridge (Phenomenex, Torrance,
533 CA, US). 5µl of sterile filtered sample were directly injected without any further manipulation.

534 Confirmation of positive metabolite identification was carried out by the acquisition of two time
535 scheduled multiple reaction monitoring (MRMs) which yielded 4.0 identification points according to
536 the European Commission decision 2002/657. In addition, retention time and ion ratio had to agree to
537 the related values of authentic standards within 0.03 min and 30% rel., respectively. Quantitation was
538 based on external calibration using serial dilutions of a multi-analyte stock solution. The accuracy of
539 the method is verified on a continuous basis by participation in a proficiency testing scheme organized
540 by BIPEA (Gennevilliers, France) with a current rate of z-scores between -2 and 2 of > 94 % (> 1300
541 results submitted).

542 RNA extraction and expression analysis

543 RNA was extracted from liquid nitrogen frozen mycelium using TRIzol Reagent (Thermo Fisher
544 Scientific). 2 µg total RNA were then subjected to DNase I digestion (Thermo Fisher Scientific). cDNA

545 was amplified using iScript™ cDNA Synthesis Kit (Bio-Rad) and LunaScript® RT SuperMix Kit (NEB). cDNA
546 was diluted 1:10 and used for qRT-PCR (Bio-Rad CFX384).

547 RNA sequencing and analysis

548 Total RNA extraction samples were transferred to Vienna Biocenter Core Facilities
549 (https://www.viennabiocenter.org/vbcf/) for library preparation and Illumina high throughput
550 sequencing using poly-A enrichment kit (NEB) and Nextera Library prep kit. 50 bp single end sequencing
551 was performed using a HiSeq v4 Illumina sequencer. Obtained sequences were de-multiplexed, quality
552 controlled , filtered using trimmomatic 0.36 (Bolger et al., 2014) and mapped on the *Aspergillus*
553 *nidulans* genome assembly (A_nidulans_FGSC_A4_version_s10-m03-r07). Mapping was performed
554 using BWA (Li and Durbin, 2009) and reverse transcripts were counted using python script HTSeq
555 (Anders et al., 2015). Normalization and statistics were done using R/Bioconductor and the limma and
556 edgeR packages, using mean-variance weighting (voom) and TMM normalisation (Law et al., 2014). A
557 significance cut-off of $p < 0.01$ was applied for analysis. Transcription levels are log2 read counts per
558 kilobase of exon per million library reads (RPKM). For trace graphs transcript coverage was calculated
559 as explained for the ChIP-seq experiments to obtain counts per million reads (CPM). All data are
560 available at NCBI GEO under the accession number GSE185285.

561 GO-enrichment analysis

562 To simplify GO interpretation we used semantic similarity measures to identify major ontologies
563 enriched in specific experiments. This means we clustered the observed GO terms based on their
564 distance in the acyclic GO-graph (Sayols et al., 2016) and extracted a common parent term.

565 NMR- measurement

566 All NMR spectra were recorded on a Bruker Avance II 400 (resonance frequencies 400.13 MHz for 1H
567 and 100.63 MHz for 13C) equipped with a N2-cooled 5 mm broadband cryoprobe head (Prodigy) with
568 z–gradients at room temperature with standard Bruker pulse programmes. The sample was dissolved
569 in 0.6 ml of MeOD (99.8 % D, Eurisotop, Saint-Aubin, France). Chemical shifts are given in ppm,
570 referenced to residual solvent signals (3.31 ppm for 1H, 49.0 ppm for 13C). 1H NMR spectrum was
571 collected with 32k complex data points whereas the 13C-jmod spectrum with WALTZ16 1H decoupling
572 was acquired using 64k data points. All two-dimensional experiments were performed with 1k × 256
573 data points, while the number of transients and the sweep widths were optimized individually. For the
574 TOCSY experiment the spin-lock time was set to 100 ms and the spinlock field to 8.3 kHz. HSQC
575 experiment was acquired using adiabatic pulse for inversion of 13C and GARP-sequence for broadband
576 13C-decoupling, optimized for 1J(CH) = 145 Hz.

577

Acknowledgements

We are grateful to Axel Brakhage and his lab members for provision of bacterial strains and critical discussion of the manuscript. Work was supported by grants from the OEAD “Sparkling Science” program (grant N° SPA 06-258) and from the Austrian Science Fund FWF, grant N° P32790-B.

608

609 ## References

610

611 Anders, S., Pyl, P.T., and Huber, W. (2015) HTSeq--a Python framework to work with high-throughput
612 sequencing data. *Bioinformatics* **31**: 166-169.
613 Ashburner, M., Ball, C., Blake, J., Botstein, D., Butler, H., Cherry, J. et al. (2000) Gene ontology: tool
614 for the unification of biology. The Gene Ontology Consortium. *Nature genetics* **25**: 25-29.
615 Bachleitner, S., Sorensen, J.L., Gacek-Matthews, A., Sulyok, M., Studt, L., and Strauss, J. (2019)
616 Evidence of a Demethylase-Independent Role for the H3K4-Specific Histone Demethylases in
617 Aspergillus nidulans and Fusarium graminearum Secondary Metabolism. *Front Microbiol* **10**: 1759.
618 Boedi, S., Berger, H., Sieber, C., Münsterkötter, M., Maloku, I., Warth, B. et al. (2016) Comparison of
619 Fusarium graminearum Transcriptomes on Living or Dead Wheat Differentiates Substrate-Responsive
620 and Defense-Responsive Genes. *Frontiers in Microbiology* **7**.
621 Boenisch, M.J., and Schäfer, W. (2011) Fusarium graminearum forms mycotoxin producing infection
622 structures on wheat. *BMC Plant Biology* **11**.
623 Bok, J.W., Chiang, Y.M., Szewczyk, E., Reyes-Domingez, Y., Davidson, A.D., Sanchez, J.F. et al. (2009)
624 Chromatin-level regulation of biosynthetic gene clusters. *Nature Chemical Biology* **5**: 462-464.
625 Bolger, A.M., Lohse, M., and Usadel, B. (2014) Trimmomatic: a flexible trimmer for Illumina sequence
626 data. *Bioinformatics* **30**: 2114-2120.
627 Bouhired, S., Weber, M., Kempf-Sontag, A., Keller, N., and Hoffmeister, D. (2007) Accurate prediction
628 of the Aspergillus nidulans terrequinone gene cluster boundaries using the transcriptional regulator
629 LaeA. *Fungal genetics and biology : FG & B* **44**: 1134-1145.
630 Brakhage, A.A. (2013) Regulation of fungal secondary metabolism. *Nat Rev Microbiol* **11**: 21-32.
631 Braus, G.H., Sasse, C., and Krappmann, S. (2006) Amino acid acquisition, cross-pathway control, and
632 virulence in Aspergillus. *Medical Mycology* **44**: 91-94.
633 Chujo, T., Lukito, Y., Eaton, C.J., Dupont, P.Y., Johnson, L.J., Winter, D. et al. (2019) Complex
634 epigenetic regulation of alkaloid biosynthesis and host interaction by heterochromatin protein I in a
635 fungal endophyte-plant symbiosis. *Fungal Genet Biol* **125**: 71-83.
636 De Boer, W., Folman, L.B., Summerbell, R.C., and Boddy, L. (2005) Living in a fungal world: Impact of
637 fungi on soil bacterial niche development. *FEMS Microbiology Reviews* **29**: 795-811.
638 de Menezes, A.B., Richardson, A.E., and Thrall, P.H. (2017) Linking fungal–bacterial co-occurrences to
639 soil ecosystem function. *Current Opinion in Microbiology* **37**: 135-141.
640 Desjardins, A.E., Hohn, T.M., and McCormick, S.P. (1993) Trichothecene biosynthesis in Fusarium
641 species: chemistry, genetics, and significance. *Microbiological Reviews* **57**: 595.

642 Doehlemann, G., Ökmen, B., Zhu, W., and Sharon, A. (2017) Plant Pathogenic Fungi. *Microbiology*
643 *spectrum* **5**.
644 Fischer, J., Müller, S.Y., Netzker, T., Jäger, N., Gacek-Matthews, A., Scherlach, K. et al. (2018)
645 Chromatin mapping identifies BasR, a key regulator of bacteria-triggered production of fungal
646 secondary metabolites. *eLife* **7**.
647 Gacek-Matthews, A., Berger, H., Sasaki, T., Wittstein, K., Gruber, C., Lewis, Z.A., and Strauss, J. (2016)
648 KdmB, a Jumonji Histone H3 Demethylase, Regulates Genome-Wide H3K4 Trimethylation and Is
649 Required for Normal Induction of Secondary Metabolism in *Aspergillus nidulans*. *PLoS Genet* **12**:
650 e1006222.
651 Gacek, A., and Strauss, J. (2012) The chromatin code of fungal secondary metabolite gene clusters.
652 *Appl Microbiol Biotechnol* **95**: 1389-1404.
653 Henke, M.T., Soukup, A.A., Goering, A.W., McClure, R.A., Thomson, R.J., Keller, N.P., and Kelleher,
654 N.L. (2016) New Aspercryptins, Lipopeptide Natural Products, Revealed by HDAC Inhibition in
655 *Aspergillus nidulans*. *ACS chemical biology* **11**: 2117.
656 Keller, N.P., Turner, G., and Bennett, J.W. (2005) Fungal secondary metabolism - from biochemistry
657 to genomics. *Nat Rev Microbiol* **3**: 937-947.
658 Klejnstrup, M.L., Frandsen, R.J.N., Holm, D.K., Nielsen, M.T., Mortensen, U.H., Larsen, T.O., and
659 Nielsen, J.B. (2012) Genetics of polyketide metabolism in *Aspergillus nidulans*. In *Metabolites*: MDPI
660 AG, pp. 100-133.
661 Law, C.W., Chen, Y., Shi, W., and Smyth, G.K. (2014) voom: Precision weights unlock linear model
662 analysis tools for RNA-seq read counts. *Genome Biol* **15**: R29.
663 Li, H., and Durbin, R. (2009) Fast and accurate short read alignment with Burrows-Wheeler
664 transform. *Bioinformatics* **25**: 1754-1760.
665 Li, Y., Tsai, K., Harvey, C., Li, J., Ary, B., Berlew, E. et al. (2016) Comprehensive curation and analysis of
666 fungal biosynthetic gene clusters of published natural products. *Fungal genetics and biology : FG & B*
667 **89**: 18-28.
668 Macheleidt, J., Mattern, D.J., Fischer, J., Netzker, T., Weber, J., Schroeckh, V. et al. (2016) Regulation
669 and Role of Fungal Secondary Metabolites. In *Annual Review of Genetics*: Annual Reviews Inc., pp.
670 371-392.
671 Margaritis, T., Oreal, V., Brabers, N., Maestroni, L., Vitaliano-Prunier, A., Benschop, J.J. et al. (2012)
672 Two distinct repressive mechanisms for histone 3 lysine 4 methylation through promoting 3'-end
673 antisense transcription. *PLoS Genet* **8**: e1002952.
674 Medema, M.H., Blin, K., Cimermancic, P., Jager, V.d., Zakrzewski, P., Fischbach, M.A. et al. (2011)
675 antiSMASH: rapid identification, annotation and analysis of secondary metabolite biosynthesis gene
676 clusters in bacterial and fungal genome sequences. *Nucleic Acids Research* **39**: W339.

677 Meng, W., and Jin, W. (1997) Structure determination of new antifungal antibiotics, polaramycins A
678 and B. *Yao Xue Xue Bao* **May;32(5)**: 352-356.
679 Nemeth, Z., Molnar, A.P., Fejes, B., Novak, L., Karaffa, L., Keller, N.P., and Fekete, E. (2016) Growth-
680 Phase Sterigmatocystin Formation on Lactose Is Mediated via Low Specific Growth Rates in
681 *Aspergillus nidulans*. *Toxins (Basel)* **8**.
682 Nislow, C., Ray, E., and Pillus, L. (1997) SET1, a yeast member of the trithorax family, functions in
683 transcriptional silencing and diverse cellular processes. *Mol Biol Cell* **8**: 2421-2436.
684 Nützmann, H.W., Reyes-Dominguez, Y., Scherlach, K., Schroeckh, V., Horn, F., Gacek, A. et al. (2011)
685 Bacteria-induced natural product formation in the fungus Aspergillus nidulans requires Saga/Ada-
686 mediated histone acetylation. *Proceedings of the National Academy of Sciences of the United States*
687 *of America* **108**: 14282-14287.
688 Oberegger, H., Schoeser, M., Zadra, I., Abt, B., and Haas, H. (2001) SREA is involved in regulation of
689 siderophore biosynthesis, utilization and uptake in Aspergillus nidulans. *Molecular Microbiology* **41**:
690 1077-1089.
691 Ogawara, H. (2016) Self-resistance in Streptomyces, with Special Reference to beta-Lactam
692 Antibiotics. *Molecules* **21**.
693 Pfannenstiel, B.T., and Keller, N.P. (2019) On top of biosynthetic gene clusters: How epigenetic
694 machinery influences secondary metabolism in fungi. *Biotechnol Adv* **37**: 107345.
695 Pontecorvo, G., Roper, J.A., Hemmons, L.M., Macdonald, K.D., and Bufton, A.W. (1953) The genetics
696 of *Aspergillus nidulans*. *Adv Genet* **5**: 141-238.
697 Pusztahelyi, T., Holb, I.J., and Pocsi, I. (2015) Secondary metabolites in fungus-plant interactions.
698 *Front Plant Sci* **6**: 573.
699 Rodriguez-Urra, A.B., Jimenez, C., Nieto, M.I., Rodriguez, J., Hayashi, H., and Ugalde, U. (2012)
700 Signaling the induction of sporulation involves the interaction of two secondary metabolites in
701 Aspergillus nidulans. *ACS Chem Biol* **7**: 599-606.
702 Rousk, J., and Bååth, E. (2007) Fungal and bacterial growth in soil with plant materials of different
703 C/N ratios. *FEMS Microbiology Ecology* **62**: 258-267.
704 Sanchez, J.F., Chiang, Y.M., Szewczyk, E., Davidson, A.D., Ahuja, M., Elizabeth Oakley, C. et al. (2010)
705 Molecular genetic analysis of the orsellinic acid/F9775 gene cluster of Aspergillus nidulans. *Molecular*
706 *BioSystems* **6**: 587-593.
707 Sayols, S., Scherzinger, D., and Klein, H. (2016) dupRadar: a Bioconductor package for the assessment
708 of PCR artifacts in RNA-Seq data. *BMC Bioinformatics* **17**: 428.
709 Schroeckh, V., Scherlach, K., Nützmann, H.W., Shelest, E., Schmidt-Heck, W., Schuemann, J. et al.
710 (2009) Intimate bacterial-fungal interaction triggers biosynthesis of archetypal polyketides in

711 *Aspergillus nidulans*. *Proceedings of the National Academy of Sciences of the United States of*
712 *America* **106**: 14558-14563.
713 Song, X., Yuan, G., Li, P., and Cao, S. (2019) Guanidine-Containing Polyhydroxyl Macrolides:
714 Chemistry, Biology, and Structure-Activity Relationship. *Molecules* **24**.
715 Strauss, J., and Reyes-Dominguez, Y. (2011) Regulation of secondary metabolism by chromatin
716 structure and epigenetic codes. *Fungal Genet Biol* **48**: 62-69.
717 Sugawara, S. (1967) Mode of action of azalomycin F. Effect of azalomycin F on Candida albicans. *The*
718 *Journal of antibiotics* **20**: 93-108.
719 Sulyok, M., Stadler, D., Steiner, D., and Krska, R. (2020) Validation of an LC-MS/MS-based dilute-and-
720 shoot approach for the quantification of > 500 mycotoxins and other secondary metabolites in food
721 crops: challenges and solutions. *Anal Bioanal Chem* **412**: 2607-2620.
722 Tag, A., Hicks, J., Garifullina, G., Ake, C., Jr., Phillips, T.D., Beremand, M., and Keller, N. (2000) G-
723 protein signalling mediates differential production of toxic secondary metabolites. *Mol Microbiol* **38**:
724 658-665.
725 Yu, J.H., and Keller, N. (2005) Regulation of secondary metabolism in filamentous fungi. In *Annual*
726 *Review of Phytopathology*, pp. 437-458.

727
728
729
730
731
732

733 **Table 1**

BGC	Up-regulated	Down-regulated	total
Derivative of Benzaldehyde1 (dba) and F9775 hybrid cluster 1 & 2	17	0	19
AN7884 (Aspercryptin)cluster	13	0	15
Terrequinone (tdi) cluster	4	0	5
Penicillin cluster	0	2	3
AN5318 cluster	2	1	5
Asperfuranone (afo) cluster	4	1	9
AN9129 cluster	1	0	2

AN9314 cluster	1	0	2
pkdA cluster	5	0	11
AN10289 cluster	2	0	5

Table 1: Selection of BGCs with differentially regulated genes (between 0 hour and 0.5 hour or between 0.5 hour and 3 hour samples). Up-regulated, Down-regulated and total refers to number of genes at least 2-fold up- or downregulated and total number of genes predicted or shown to belong the given cluster, respectively.

761 **Figures**

762 Figure 1

763

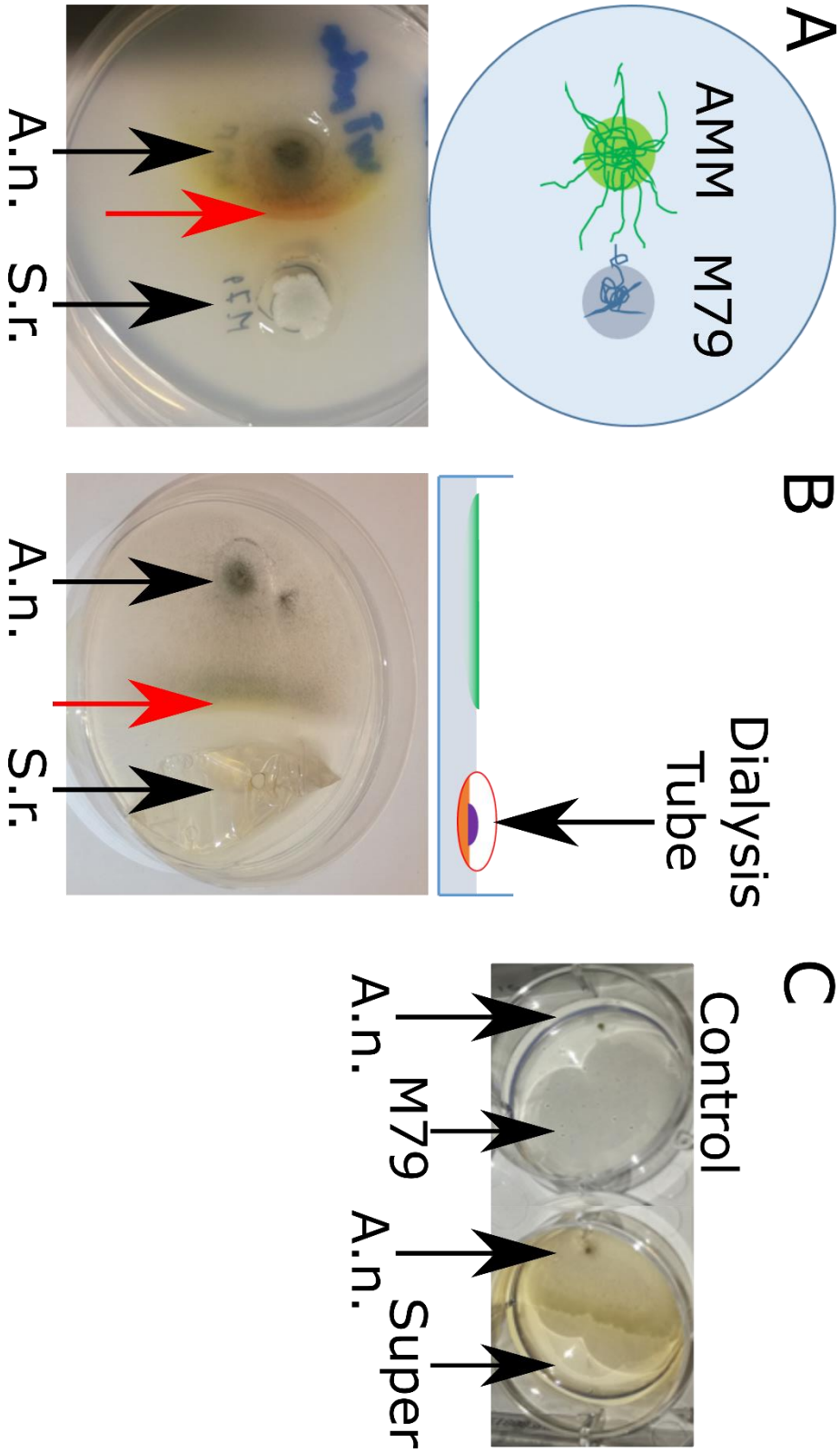

764

765

766 **Figure 1: A**: Top: Schematic setup; Aspergillus minimal medium (AMM) and M79 medium was placed
767 into phosphate buffered water agar (green and blue circles, respectively). AMM and M79 media
768 were inoculated with *A. nidulans* (A.n.) and *S. rapamycinicus* (S.r.), respectively, and incubated for 7
769 days at 30°C. Bottom: Yellow pigments (YPs) production, (red arrow) of *A. nidulans* growing on
770 phosphate buffered water agar towards *S. rapamycinicus* colonies.

771 **B**: Top: Schematic setup; similar as Figure 1A, except that *S. rapamycinicus* was inoculated into a
772 dialysis tube partially filled with M79 medium thus preventing physical contact with *A. nidulans* cells
773 from the confronting fungal colony. Bottom: red arrow points to the YPs that can also be observed in
774 this setup after 7 days at 30°C, although to a lesser extent. **C**: 10µl of media supernatant (Super) from
775 *S. rapamycinicus* grown "solo" in liquid M79 for 7 days at 30°C, was applied opposite to a growing *A.*
776 *nidulans* colony (6 well plate) and a clear YPs production was observed.

777
778
779
780
781
782
783
784
785
786
787
788
789
790
791
792
793
794
795
796
797

Figure 2

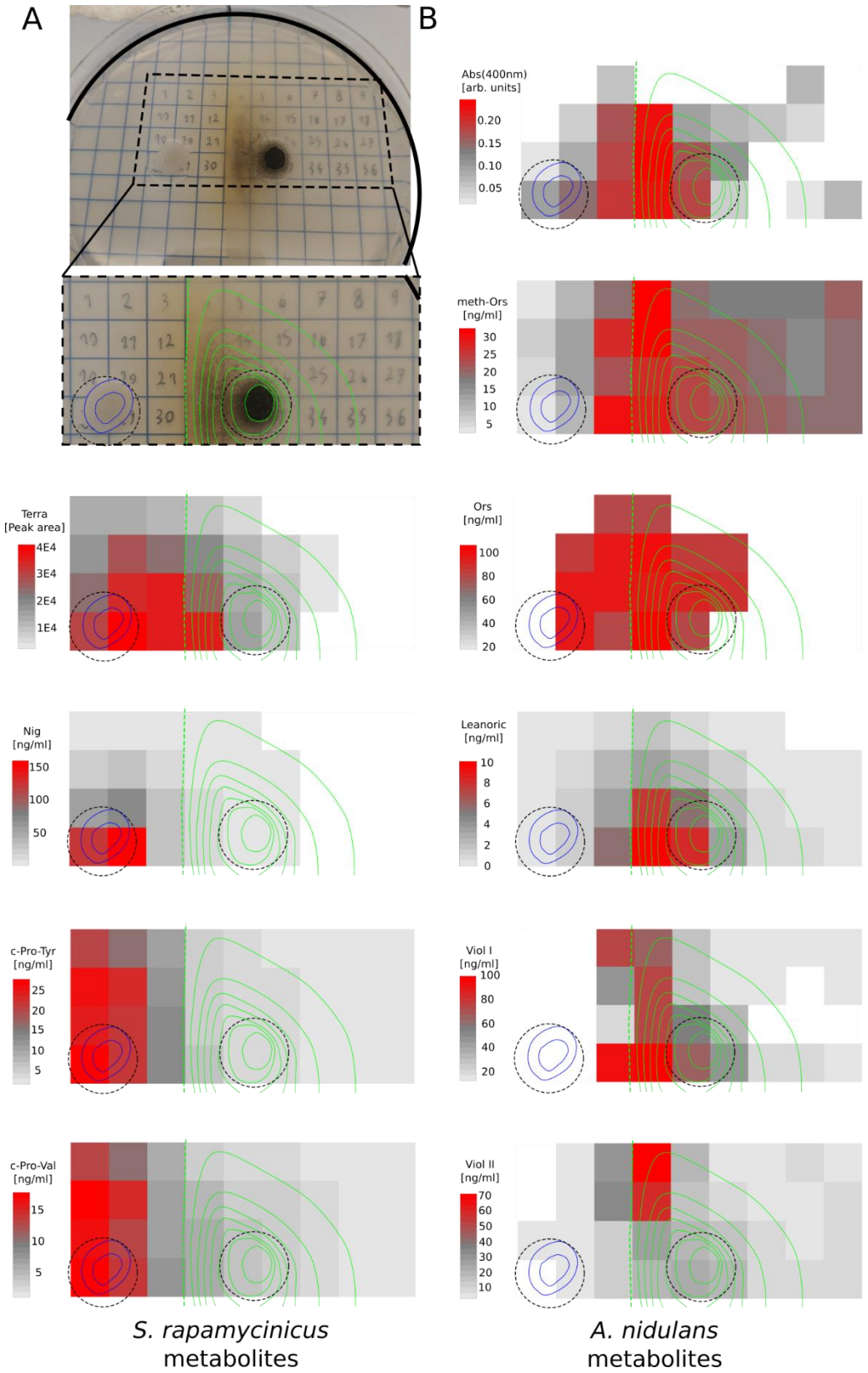
A
B
Abs(400nm)
[arb. units]
0.20
0.15
0.10
0.05
meth-Ors
[ng/ml]
30
25
20
15
10
5
Terra
[Peak area]
4E4
3E4
2E4
1E4
Ors
[ng/ml]
100
80
60
40
20
Nig
[ng/ml]
150
100
50
Leanoric
[ng/ml]
10
8
6
4
2
0
c-Pro-Tyr
[ng/ml]
25
20
15
10
5
Viol I
[ng/ml]
100
80
60
40
20
c-Pro-Val
[ng/ml]
15
10
5
Viol II
[ng/ml]
70
60
50
40
30
20
10
S. rapamycinicus
metabolites
A. nidulans
metabolites

802 **Figure 2. A:** Top/Left: Experimental setup with an example of the confrontation assay on agar plates
803 and a magnified section of it below the plate photograph. The raster with numbers represent areas
804 that were cut out from the agar and analyzed by mass spectrometry (see materials and methods).
805 Growing *S. rapamycinicus* cells are indicated by blue line circled areas, the *A. nidulans* colony is
806 indicated by green line circled areas; dotted green line shows the extent of fungal growth (complete
807 right hand side of plate is covered by fine mycelia. Dotted black circles indicate the areas of AMM or
808 M79 media in the plate. Conidiation is strongest in the region facing the *S. rapamycinicus* colony.
809 Heatmaps show metabolite concentrations found in the respective regions, positions of colonies are
810 indicated by blue and green lines. Below the photograph in panel A, heatmaps are shown that
811 represent metabolite concentrations found in the respective region originating from *S.*
812 *rapamycinicus*.

813 **B:** Heatmaps representing metabolite concentrations of the *A. nidulans* colony. Absorption (400nm)
814 representing YPs. Levels of other *A.nidulans* metabolites are shown as separate heatmeaps.
815 Abbreviations: Terra: terragine: Ors: orsellinic acid; Lecanoric: lecanoric acid; meth-Ors:
816 methylorsellinic acid; Viol I: violaceol I; Viol II: violaceol II; Nig: nigericin.

817

818

819

820

821

822

823

824

825

826

827

828

829

830

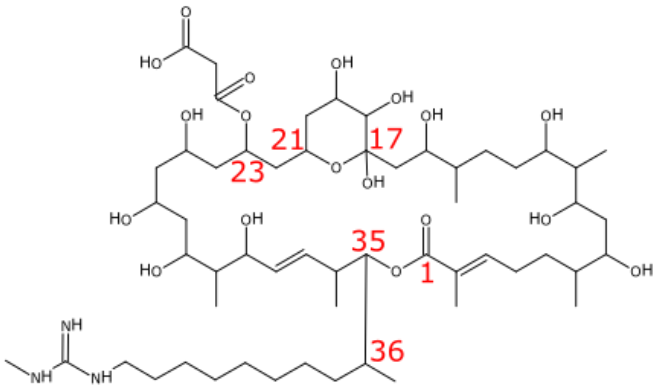

Figure 3. Structure of PolaramycinB. The C17-C21 hemiketal ring has been shown to be important for antimicrobial activity, whereas C23 malonyl reduced antimicrobial activity.

847 Figure 4

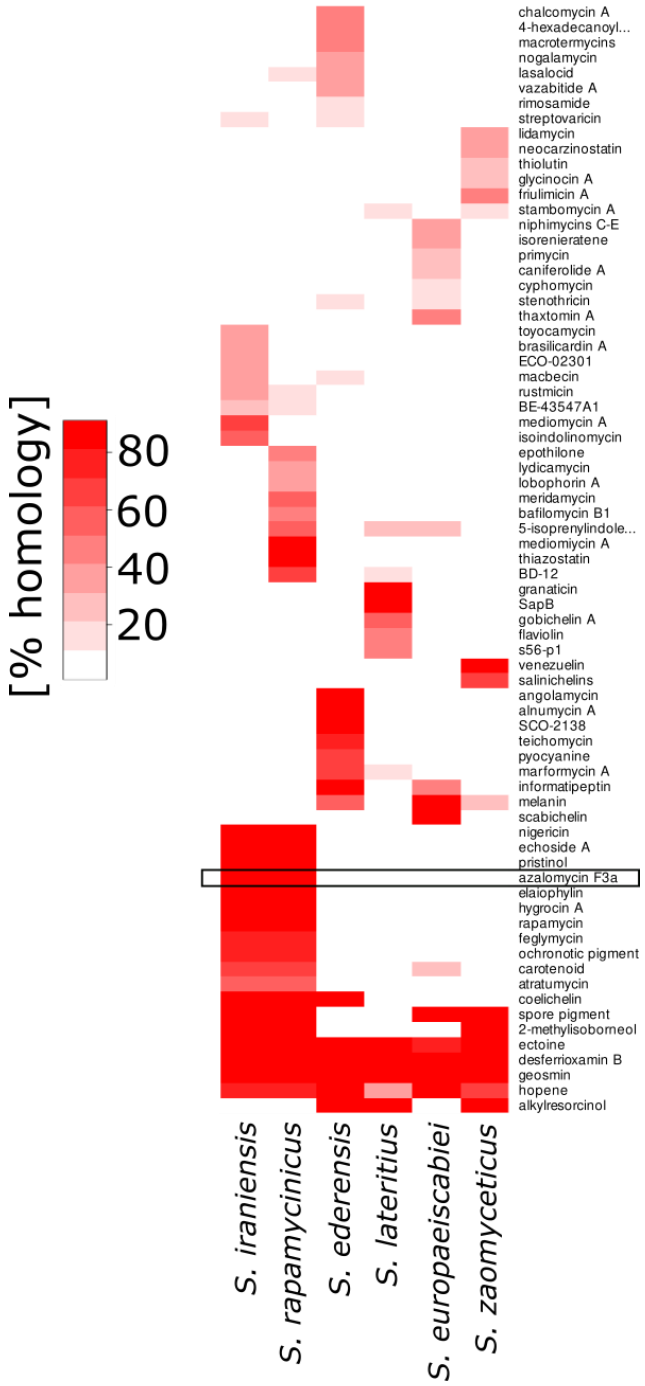

848

849

850 **Figure 4.** Homology search (anti-SMASH) in *S. rapamycinicus*, *S. iraniensis*, *S. zaomyceticus*, *S.*
851 *ederensis*, *S. lateritius* and *S. europaeiscabiei* for putative secondary metabolite clusters. Only *S.*
852 *rapamycinicus* and *S. iraniensis* induce YPs, both containing a homologous azalomycin F3a gene
853 cluster (black box). Red color indicates percent homology.

854

855

856 Figure 5

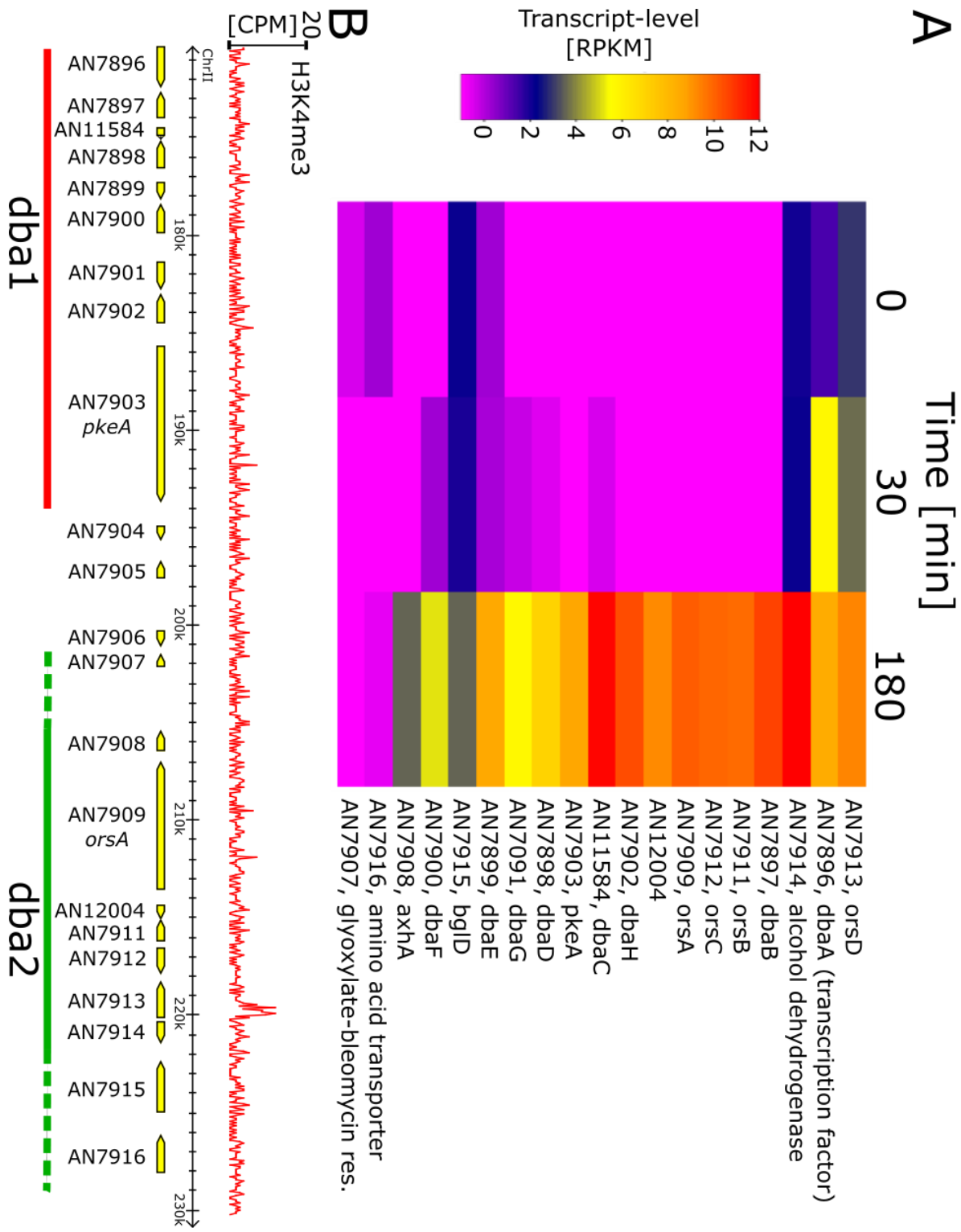

857

858 **Figure 5**: **A**. Color coded transcript levels (RPKM) of dba cluster genes, columns represent time after
859 polaramycin B treatment. Gene names or descriptions are shown if available. The transcription factor
860 *dbaA* is already induced after 30 minutes following treatment, what seems not to be the case for the
861 remaining cluster genes, that are induced at the later time point, presumably only after the
862 transcription factor protein DbaA was translated and activated. AN7916 and AN7907 are not induced
863 at all and may not be part of the dba-cluster. **B:** Genome and chromatin organization of both dba1

and dba2 derivative of Benzaldehyde1 gene clusters. Red graph shows histone H3K4 methylation after 18 hours, taken from (Gacek-Matthews *et al.*, 2016), a single significant peak found in AN7913.

Figure 6

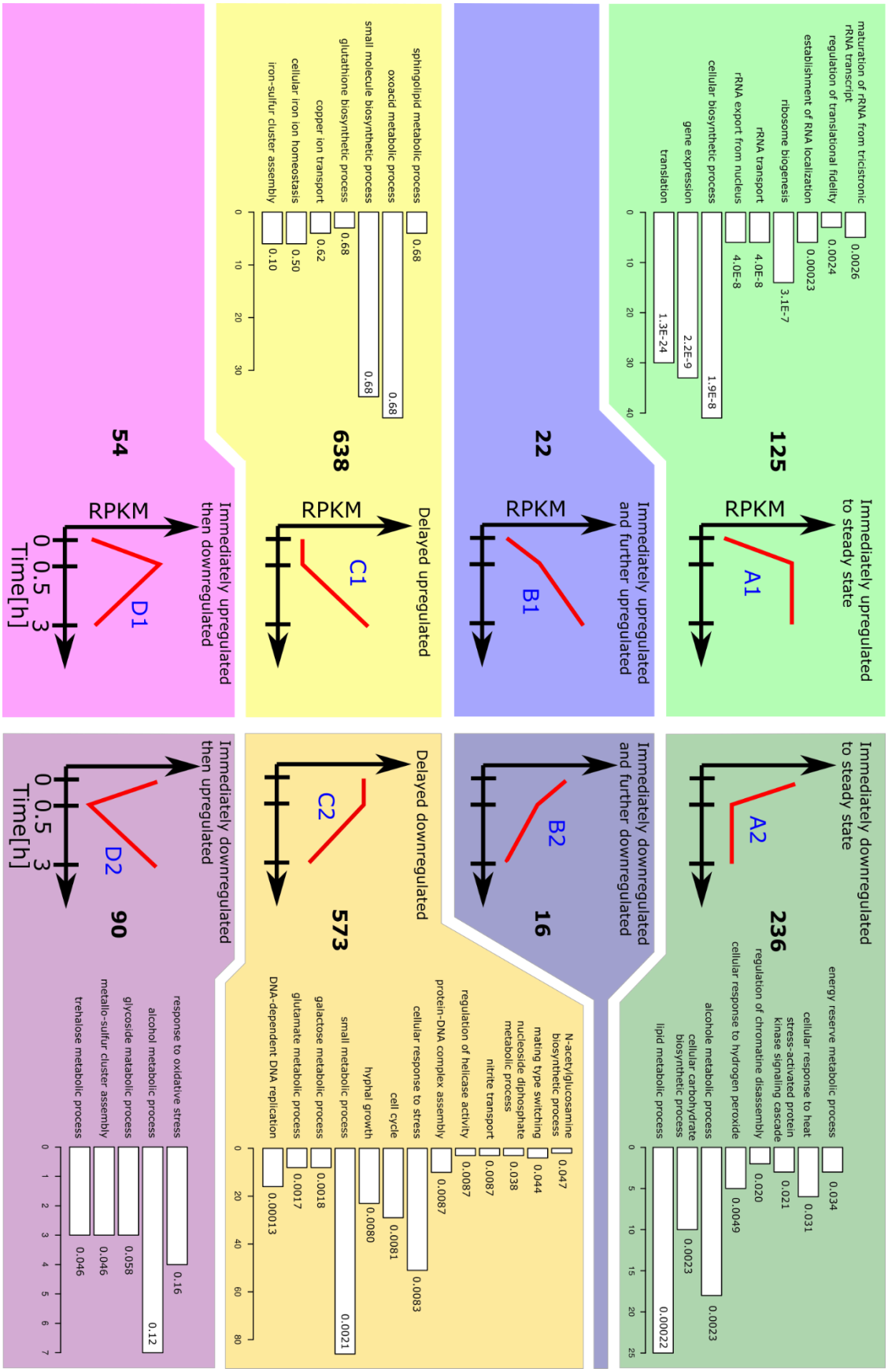
Immediately upregulated to steady state
125
RPKM
A1
maturation of rRNA from tricistronic rRNA transcript
regulation of translational fidelity
establishment of RNA localization
ribosome biogenesis
rRNA transport
rRNA export from nucleus
cellular biosynthetic process
gene expression
translation
0.0026
0.0024
0.00023
3.1E-7
4.0E-8
4.0E-8
1.9E-8
2.2E-9
1.3E-24
0
10
20
30
40
Immediately upregulated and further upregulated
22
RPKM
B1
Delayed upregulated
638
RPKM
C1
sphingolipid metabolic process
oxoacid metabolic process
small molecule biosynthetic process
glutathione biosynthetic process
copper ion transport
cellular iron ion homeostasis
iron-sulfur cluster assembly
0.68
0.68
0.68
0.62
0.50
0.10
0
10
20
30
Immediately downregulated then downregulated
54
RPKM
D1
0 0.5 3
Time[h]
Immediately downregulated to steady state
236
RPKM
A2
energy reserve metabolic process
cellular response to heat
stress-activated protein kinase signaling cascade
regulation of chromatine disassembly
cellular response to hydrogen peroxide
alcohole metabolic process
cellular carbohydrate biosynthetic process
lipid metabolic process
0.034
0.031
0.021
0.020
0.0049
0.0023
0.0023
0.00022
0
5
10
15
20
25
Immediately downregulated and further downregulated
16
RPKM
B2
N-acetylglucosamine biosynthetic process
mating type switching
nucleoside diphosphate metabolic process
nitrite transport
regulation of helicase activity
protein-DNA complex assembly
0.047
0.044
0.038
0.0087
0.0087
0.0083
Delayed downregulated
573
RPKM
C2
cellular response to stress
cell cycle
hyphal growth
small metabolic process
galactose metabolic process
glutamate metabolic process
DNA-dependent DNA replication
0.0081
0.0080
0.0021
0.0018
0.0017
0.00013
0
20
40
60
80
Immediately downregulated then upregulated
90
RPKM
D2
0 0.5 3
Time[h]
response to oxidative stress
alcohol metabolic process
glycoside metabolic process
metallo-sulfur cluster assembly
trehalose metabolic process
0.16
0.12
0.058
0.046
0.046
0
1
2
3
4
5
6
7

892 **Figure 6.** Gene-set clustering of induction kinetiks in response to Polaramycin B at 3 time points. The
893 combination of a p-value < 0.01 and a differential expression of ±1 was condidered a significant
894 differential expression. y-axses of diagramms show transcript levels, x-axes represent time. Total
895 number of genes in each clustered gene-set are shown in bold numbers, barplots show GO-term
896 enrichments, bar-length represent number of genes, number within barplots show corrected p-
897 values.

898

899